

# Propagation of uncertainty in multi-matrix analysis by GD-OES

Zdeněk Weiss

LECO Instrumente Plzeň, spol.s r.o., Plaská 66, 323 25 Plzeň, Czech Republic.  
E-mail: weissz@leco.cz

Received 12th July 2001, Accepted 7th September 2001  
First published as an Advance Article on the web 11th October 2001

www.rsc.org/jaas

Propagation of uncertainty was analysed in multi-matrix calibrations by GD-OES and a formalism was developed to calculate uncertainties of the calibration parameters, sputter factors and the predicted concentrations in the standard model. This formalism is intended for evaluation of the analytical performance of different experimental setups and as a basis for further developments of the calibration model. In this work, it was applied to a multi-matrix calibration covering a wide range of mostly nickel-based alloys. Evidence was found that deviations from the standard model exist in that calibration. Typical levels of uncertainty to be expected in the multi-matrix analysis by GD-OES are presented.

## 1. Introduction

A well-known and highly valued feature of GD-OES is its capability to analyse a wide range of materials (matrices) using a single calibration. Methodology of such analyses is based on a semi-empirical concept called *matrix-independent emission yields*.<sup>1–3</sup> Mathematical description of this concept was developed as a self-consistent formalism, describing relations between emission line intensities and composition of the analysed materials. It is sometimes referred to as the ‘standard model’ of GD-OES.<sup>4–7</sup> The expression ‘standard model’ should not be understood as being a model formally adopted as a standard by ISO or another similar body. The standard model has been remarkably successful, especially for metals, delivering a very good analytical performance in many applications.

This statement, however, may be considered somewhat vague if the analytical performance is not evaluated exactly. Also, it is well known that, in certain situations, the standard model does not describe reality accurately enough and various modifications and additional corrections are being proposed.<sup>8–11</sup> In such developments, it is vital to evaluate and compare analytical performances of different quantification models, excitation methods, discharge stabilization modes, *etc.* To do all of this, analytical performance should be evaluated exactly, which is not possible without considering the uncertainty associated with the data. So far, no systematic attention has been paid to the problem of uncertainty in GD-OES analysis. It is a goal of this paper to analyse uncertainty propagation in the standard model of GD-OES and develop tools to estimate the random- and prospective systematic errors in all stages of the analysis.

## 2. Theoretical considerations

### 2.1. Flow of information in GD-OES analysis

Discussion of uncertainty propagation in this paper covers the standard model of GD-OES with a linear intensity response, as described in refs. 4–6. The non-linear intensity response, treated in ref. 7, is not explicitly discussed here under ‘Theoretical considerations’ because the extension of the theory is straightforward. However, the data presented under ‘Experimental’ were treated with an uncertainty propagation formalism in which the non-linear intensity response was included.

In a typical GD-OES experiment, intensities of selected

emission lines of analysed elements are recorded simultaneously for the samples excited in the glow discharge excitation source. In the standard model of GD-OES, the relation between the emission intensities and the sample composition is supposed to be the following:

$$I_{E,M} = R_E q_M c_{E,M} + \sum_F \alpha_{EF} I_{F,M} + b_E \quad (1)$$

where  $M$  is the index distinguishing between different samples (matrices)†;  $E$  is the index distinguishing between different elements (emission lines);  $I_{E,M}$  is the intensity of a line of the element  $E$  in a matrix  $M$ ;  $c_{E,M}$  is the concentration of the element  $E$  in the matrix  $M$ ;  $R_E$  is called the *emission yield*;  $b_E$  is the term expressing the *spectral background*;  $\alpha_{EF}$  is the *interference correction factor* for a disturbing element  $F$ ; and  $q_M$  is called the *sputter rate factor*.

It is supposed that (1) the quantities indexed by  $E$  only (*e.g.*,  $R_E$ ,  $b_E$ ) are characteristic to the element (emission line) and do not depend on the matrix, and (2) that the sputter rate factors,  $q_M$ , indexed only by  $M$ , depend on the matrix and not on the element (emission line). Interference correction factors,  $\alpha_{EF}$ , are characteristic of the pair of elements  $E$ ,  $F$  and supposedly do not depend on the matrix.  $I_{E,M}$  and  $c_{E,M}$  are the variables and  $R_E$ ,  $b_E$  and  $\alpha_{EF}$  are intrinsic parameters (constants) of the model.  $R_E$ ,  $b_E$  and  $\alpha_{EF}$  are specific to each particular experiment (*i.e.*, they depend, for example, on the detector sensitivities and other instrumental parameters). They are determined experimentally by calibration. The sputter rate factors are defined as such factors that make the values  $I_{E,M}$  and  $c_{E,M}$  consistent with eqn. (1). Obviously, such a definition is reasonable as long as the standard model holds true, but becomes problematic when the model is violated by matrix effects.<sup>4,11</sup> A further discussion of this point follows below. The parameters of the calibration are calculated by regression, minimizing the error function (chi-squares function) corresponding to eqn. (1):

$$\chi^2 = \sum_M \sum_E \omega_{E,M} (I_{E,M} - R_E q_M c_{E,M} - \sum_F \alpha_{EF} I_{F,M} - b_E)^2 \quad (2)$$

where  $\omega_{E,M}$  is the statistical weight associated with the analysis of the element  $E$  in the sample  $M$ .

†The expressions *matrix* and *sample* are sometimes used interchangeably throughout the paper.

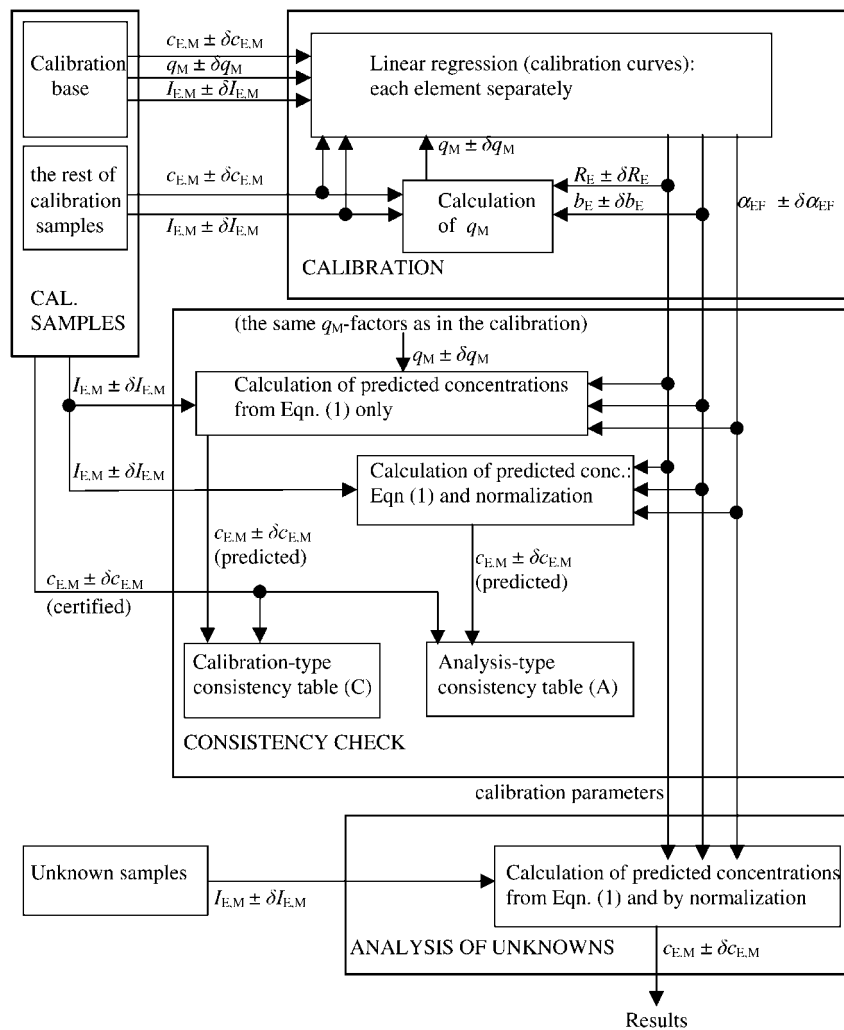


Fig. 1 Flow of information in a GD-OES analysis.

A schematic of the flow of information in a GD-OES analysis is given in Fig. 1. Calibration samples are measured first and the corresponding emission intensities are collected. Calibration parameters for at least some elements are calculated, based on a sub-set of all calibration samples for which the sputter factors are known. This sub-set, together with those elements, is called the *calibration base*. In multi-matrix calibrations, some calibration samples are usually needed to cover the requested concentration ranges, for which the sputter factors are unknown. Sputter factors of such samples must first be calculated, using the normal equation for  $q_M$  associated with the error function, eqn. (2):

$$\sum_E \omega_{E,M} R_E c_{E,M} (I_{E,M} - R_E q_M c_{E,M} - \sum_F \alpha_{E,F} I_{F,M} - b_E) = 0 \quad (3)$$

In the above equation,  $E$  runs only through the elements of the calibration base and  $R_E$ ,  $b_E$  and  $\alpha_{EF}$  are constants known from the previous step.<sup>4,5</sup>

Suppose that the method has been calibrated and the calibration parameters  $R_E$ ,  $b_E$  and  $\alpha_{EF}$  are known for all elements, then the composition of an unknown sample still cannot be calculated simply from eqn. (1) because its sputter factor,  $q_M$ , is not known. To overcome this, it is assumed that all elements present in the sample at measurable concentrations have been analysed and the sum of their concentrations is 1 (*i.e.*, 100%: weight fractions are used here). Using eqn. (1), this gives the following formula for  $q_M$ :

$$q_M = \frac{\sum_E (I_{E,M} - \sum_F \alpha_{EF} I_{F,M} - b_E)}{R_E} \quad (4)$$

The unknown concentration,  $c_{EM}$ , can then be calculated by substituting this into eqn. (1):

$$c_{EM} = \frac{I_{E,M} - \sum_F \alpha_{EF} I_{F,M} - b_E}{R_E \sum_G (I_{G,M} - \sum_F \alpha_{GF} I_{F,M} - b_G) / R_G} \quad (5)$$

The above procedure is referred to as ‘normalization’. It is worth mentioning that, unlike the case in which the sputter factor is known, the predicted concentration,  $c_{EM}$ , depends on the intensities of all analysed elements through the denominator in eqn. (5).

A discussion of the intermediate step, *i.e.*, the consistency check of the method, remains. As mentioned above, the standard model does not always reflect the whole complexity of the glow discharge excitation. Hence, even if extending the model to cover resonance lines with non-linear intensity response, certain discrepancies may still exist between the predicted and the ‘true’ concentrations. Such discrepancies are attributed to matrix effects. There are two common ways of suppressing the matrix effects: 1, to modify the model by introducing additional *ad hoc* parameters; and 2, to narrow the analytical range.

Magnitude of the matrix effects and accuracy of the method can be evaluated. Take a table in which rows represent the

calibration samples and columns represent the elements (emission lines) and each cell contains the deviation between the 'predicted' and the 'true' concentration. Let this table be called the *consistency table*. As can be inferred from Fig. 1, two types of consistency tables are suggested, differing in the way in which the sputter factors are treated. For the calibration-type (C-type) consistency table, the predicted concentrations are calculated directly from eqn. (1), with the same  $q_M$  values as used in the calibration. For the analysis-type (A-type) consistency table, the predicted concentrations are calculated in the same way as for the unknown samples, *i.e.*, sputter factors are calculated by normalization.

Clearly, the A-type consistency table reflects the overall accuracy of the method and can be directly used to evaluate the analytical performance. The C-type calibration table contains more information about the model itself.

## 2.2. Propagation of uncertainty in GD-OES analysis

According to the previous paragraph, GD-OES analysis can be described as a sequence of steps, in each of which some quantities are known (input) and others are calculated (output). The goal is to analyse uncertainties associated with these quantities in the complete chain of the transformations. Because of the complexity, estimated uncertainties are calculated step-by-step, together with the corresponding parameters and variables and within the same computer program, so that the calculations can be controlled interactively (*e.g.*, by selecting the calibration base). In this section, uncertainty propagation in each step is discussed.

**2.2.1. Calibration: intrinsic calibration parameters  $R_E$ ,  $b_E$ ,  $\alpha_{EF}$ .** Uncertainties of the calibration parameters  $R_E$ ,  $b_E$  and  $\alpha_{EF}$  determine the magnitude of the systematic errors within the standard model. Because of the complexity, explicit formulae for  $\delta R_E$ ,  $\delta b_E$  and  $\delta \alpha_{EF}$  as functions of  $\delta c_{EM}$ ,  $\delta q_M$ ,  $\delta I_{EM}$  and  $\delta I_{FM}$  are not discussed here. However, these uncertainties have been calculated when treating the experimental data.

For illustration, explicit formulae for  $\delta R_E$  and  $\delta b_E$  are given for a simplified case in which  $\alpha_{EF}=0$  and  $\omega_{EM}=1$ :

$$(\delta b_E)^2 = \frac{\sum_M \Delta_{EM}^2}{N-2} \cdot \frac{\sum_M c_{EM}^2 q_M^2}{N \cdot \sum_M c_{EM}^2 q_M^2 - \left( \sum_M c_{EM} q_M \right)^2} \quad (6)$$

$$(\delta R_E)^2 = \frac{\sum_M \Delta_{EM}^2}{N-2} \cdot \frac{N}{N \cdot \sum_M c_{EM}^2 q_M^2 - \left( \sum_M c_{EM} q_M \right)^2} \quad (7)$$

where

$$\Delta_{EM}^2 = (\delta I_{EM})^2 + R_E^2 [c_{EM} \delta q_M + \delta c_{EM} q_M]^2 \quad (8)$$

and  $N$  is the number of calibration samples.

**2.2.2. Calibration: calculation of  $q_M$ .** In this step eqn. (3) is used. It can be re-written, so that  $q_M$  is expressed as a function of the other parameters. To get good estimates of  $q_M$ , let only lines unaffected by line interferences enter the calibration base and only experimental points with intensities well above the background be used. Hence, the following assumption is made to simplify the calculations:  $b_E=0$  and  $\alpha_{EF}=0$ . From the general rule for propagation of independent and random errors,<sup>12</sup> the following estimate of the uncertainty of  $q_M$  can be

derived:

$$(\delta q_M)^2 = \frac{\sum_E \omega_{EM}^2 I_{EM}^2 [(\delta R_E)^2 c_{EM}^2 + (\delta c_{EM})^2 R_E^2 + (\delta I_{EM})^2 / q_M^2]}{\sum_E \omega_{E,M} (R_E c_{EM})^2} \quad (9)$$

In this expression, index  $E$  runs only through the elements of the calibration base.

**2.2.3. The C-type consistency check.** The C-type consistency check involves calculation of the predicted concentrations directly from eqn. (1). Sputter factors and their uncertainties are treated as known quantities. Uncertainties of the concentrations are then given by:

$$\left( \frac{\delta c_{EM}}{c_{EM}} \right)^2 = \left( \frac{\delta R_E}{R_E} \right)^2 + \left( \frac{\delta q_M}{q_M} \right)^2 + \frac{(\delta I_{EM})^2 + (\delta b_E)^2 + \sum_F [I_{FM}^2 (\delta \alpha_{EF})^2 + \alpha_{EF}^2 (\delta I_{FM})^2]}{c_{EM}^2 R_{EM}^2 q_M^2} \quad (10)$$

**2.2.4. Analysis of unknown samples and the A-type consistency check.** An attempt to express the uncertainty,  $\delta c_{E,M}$ , as a function of the uncertainties of all variables and parameters of eqn. (5) would result in a very complex formula. Instead, two important special cases are discussed, showing the general behavior of  $\delta c_{E,M}$ .

*High and medium concentrations, not very severe line interferences.* In this case, the emission intensity of each analytical line is mostly related to the corresponding element sputtered from the sample, *i.e.*, the measured intensities are much stronger than their components coming from line interferences and the background. The error,  $\delta c_{E,M}$ , will then be caused by uncertainties of the measured intensities and the emission yields. Using general rules of uncertainty propagation, the following equation can be derived from eqn. (5) if the uncertainties are random and independent:

$$\left( \frac{\delta c_{EM}}{c_{EM}} \right)^2 = (1 - c_{EM})^2 \left[ \left( \frac{\delta I_{EM}}{I_{EM}} \right)^2 + \left( \frac{\delta R_E}{R_E} \right)^2 \right] + \sum_{G \neq E} c_{GM}^2 \left[ \left( \frac{\delta I_{GM}}{I_{GM}} \right)^2 + \left( \frac{\delta R_G}{R_G} \right)^2 \right] \quad (11)$$

In multiple analyses of a single sample, only intensities are changing, *i.e.*, in each square bracket the first term represents the random error and the second term the systematic error due to the biased emission yields (calibration parameters) used for the calculations, *i.e.*, the systematic error within the standard model. From the above formula, the following conclusions can be inferred: 1, contributions to the relative error of  $c_{E,M}$  caused by errors in intensities and emission yields of the other elements are proportional to their concentrations; and 2, at high concentrations of the element  $E$  (close to 1), contributions to  $\delta c_{E,M}/c_{E,M}$  from  $\delta I_{E,M}$  and  $\delta R_E$  are suppressed by normalization and contributions from the other elements are small because their concentrations are small. Hence, for materials consisting mostly of a single element, the relative error of that element will be small, no matter how big the errors of the intensities and the calibration constants are.

It is worth mentioning that the assumption that the errors,  $\delta I_{E,M}$  and  $\delta I_{G,M}$ , are random and independent is crucial; frequently a substantial part of the intensity variations comes from a variable sputter rate of the matrix. In such a case,  $\delta I_{E,M}$  and  $\delta I_{G,M}$  are highly correlated, a substantial cancellation of the errors occurs and eqn. (11) significantly overestimates the actual error.

*Low concentrations.* A typical magnitude of relative errors of concentrations due to the uncertainty in the sputter factor, *i.e.*, errors introduced by normalization, is a few percent at most. However, in the limit of low analyte concentrations, relative errors to be expected are much larger. Hence, it will probably be better to neglect the term related to  $\delta q_M$ , rather than to examine what  $\delta q_M$  depends on, and, consequently, it is better to start with eqn. (10) instead of eqn. (5). Also the relative contribution of  $\delta R_E$  to the error of concentration will be small for small concentrations. Hence, the first two terms in eqn. (10) can be neglected.

Let the quantities  $(BEC)_E$  and  $(IEC)_{EF}$  be introduced as:

$$b_E = (BEC)_E R_{EQM} \quad (12)$$

$$\alpha_{EF} q_M R_F = (IEC)_{EF} R_{EQM} \quad (13)$$

Eqn. (10) can then be re-written as:

$$(\delta c_{EM})^2 = \frac{(\delta I_{EM})^2}{R_E^2 q_M^2} + \left(\frac{\delta b_E}{b_E}\right)^2 (BEC)_E^2 + \sum_F \left[ \left(\frac{\delta \alpha_{EF}}{\alpha_{EF}}\right)^2 + \left(\frac{\delta I_{FM}}{I_{FM}}\right)^2 \right] c_{FM}^2 (IEC)_{EF}^2 \quad (14)$$

$(BEC)_E$  is called the background-equivalent concentration of the element  $E$ , and, by analogy,  $(IEC)_{EF}$  is called the interference-equivalent concentration and represents the apparent contribution to the concentration of the element  $E$  caused by the interfering element  $F$  if the concentration of the element  $F$  in the matrix is 1 (=100%). The quantity  $(IEC)_{EF}$  is dimensionless and represents the above mentioned apparent concentration as a mass fraction. In eqn. (14), random error is represented by the terms containing  $\delta I_{EM}$  and  $\delta I_{FM}$ . The other terms represent systematic errors within the standard model, due to the biased calibration parameters  $b_E$  and  $\alpha_{EF}$ . In eqn. (14) in the square bracket,  $\delta I_{FM}/I_{FM}$  is usually small compared to  $\delta \alpha_{EF}/\alpha_{EF}$ . As far as the first term of eqn. (14) is concerned, in the limit of very low analyte concentrations,  $I_{EM}$  consists only of the background and the spectral interferences. The background-related term is already included in eqn. (14), so  $\delta I_{EM}$  can be regarded as originating just from the interferences. Under such assumptions, eqn. (14) gives:

$$(\delta c_{EM})^2 = \left(\frac{\delta b_E}{b_E}\right)^2 (BEC)_E^2 + \sum_F \left[ \left(\frac{\delta \alpha_{EF}}{\alpha_{EF}}\right)^2 + \left(\frac{\delta I_{EF}}{I_{EF}}\right)^2 \right] c_{FM}^2 (IEC)_{EF}^2 \quad (15)$$

where  $I_{EF}$  is the contribution to the intensity  $I_{EM}$  caused by the element  $F$ . This equation can be used, for example, to estimate the limit of detection of the element  $E$  in different matrices. It is worth mentioning that the systematic errors caused by biased interference correction factors,  $\alpha_{EF}$ , may become very significant at low concentrations, hence, it is important to determine the  $\alpha_{EF}$  parameter as accurately as possible.

### 2.3. Accuracy and the matrix effects

Consistency tables as defined under 2.1 may be used to check the accuracy of the method. Any value in the consistency table (deviation) that significantly exceeds the uncertainty associated with the corresponding cell of the consistency table indicates an inconsistency. By 'uncertainty' we mean here the random and systematic uncertainties of the measurement, combined with the uncertainty of the corresponding certified concentration.

In practice, with a reasonably good instrument performance and using typical certified reference materials, it is almost impossible to achieve a full self-consistency within the standard model. Therefore, and also for the purpose of comparison with

other methods, it would be desirable to define parameters describing the 'magnitude of matrix effects'.

In ref. 13 there is such a quantity, called the standard error ( $SE$ ). For an element  $E$ , it is defined as:

$$(SE)_E = \sqrt{\frac{1}{f} \sum_M [c_{EM}(\text{certified}) - c_{EM}(\text{predicted})]^2} \quad (16)$$

where  $f$  is degrees of freedom, *i.e.*, the number of calibration samples defining the calibration curve for the element  $E$  minus the number of calibration parameters corresponding to that curve. However, this definition is not very suitable for large concentration ranges spanning over several orders of magnitude, common in multi-matrix applications. Also, the standard error  $SE$  tends to give rather conservative estimates, *i.e.*, depends strongly on the largest deviation among all relevant calibration samples.

In this paper, a quantity  $\varepsilon(c)$  is introduced that describes the 'typical relative uncertainty' to be expected if analysing the concentration  $c$  by other common methods.  $\varepsilon(c)$  is defined below as a power function of concentration, namely as a linear least-squares fit of the uncertainties of the certified concentrations, plotted against the certified concentrations in the logarithmic scale:

$$\log \varepsilon(c) = k_1 \log c + k_2 \quad (17)$$

where  $k_1 = -0.401$  and  $k_2 = 0.191$ .

The set of certified reference materials used to define this function is listed in Table 1 and the uncertainties, coming from the certificates, are plotted against the certified concentrations in Fig. 2, together with a straight line representing the function  $\varepsilon(c)$ .

With the function  $\varepsilon(c)$ , the following quantities can be used to characterize deviations of the experimental points from the standard model in a wide concentration range:

$$(ERR)_{EM} = \frac{c_{EM}(\text{certified}) - c_{EM}(\text{predicted})}{\varepsilon(c_{EM}(\text{certified}))} \quad (18)$$

The quantity

$$(ERR)_E = \text{Median}_M \{ |(ERR)_{EM}| \} \quad (19)$$

characterizes then how consistent the calibration curve of the element  $E$  is with the standard model.

There is one more advantage in using the function  $\varepsilon(c)$ : GD-OES measurements tend to be heteroscedastic, *i.e.*, the random uncertainty associated with the measurements depends on the analysed concentration. The random uncertainty increases with decreasing concentration, in a similar manner to  $\varepsilon(c)$ , hence expressing the total uncertainty in the units of  $\varepsilon(c)$  makes it easy to check the observed deviations for statistical significance.

## 3. Experimental

Uncertainty propagation was studied for a multi-matrix calibration specifically developed for the analysis of various nickel, iron and cobalt based alloys. A list of the calibration samples is given in Table 1. The measurements were made using the LECO SA-2000 GD-OES spectrometer, described elsewhere.<sup>7</sup> The particular instrument used was not configured specifically for this application, and, for some elements, better lines may exist for the analysis of nickel alloys than those reported here.

Dc glow discharge was used for excitation, operating in the mode of dynamic pressure control, with a stabilized voltage of 800 V and a constant current of 30 mA. To suppress a prospective instrument drift, the calibration was measured five times, each time with one analysis per sample. After that, the measurements corresponding to the same sample were grouped

**Table 1** List of the calibration samples with certified concentrations (weight %)

	Grade	Fe	C	P	S	Mn	Si	Ni	Cr	Cu	Mo	Co	Ti	V	Al	B	Nb	W
1761	Low alloy steel	95.0	1.03	0.04	0.035	0.678	0.18	1.99	0.22	0.30	0.103	0.028	0.18	0.053	0.055	0.002	0.021	
1762	Low alloy steel	94.1	0.337	0.033	0.03	2.00	0.35	1.15	0.92	0.12	0.35	0.062	0.095	0.20	0.069	0.0049	0.07	
1763	Low alloy steel	95.0	0.203	0.012	0.023	1.58	0.63	0.51	0.50	0.043	0.50	0.095	0.31	0.30	0.043	0.0054	0.10	
1764	Low alloy steel	95.5	0.592	0.02	0.012	1.21	0.057	0.202	1.48	0.51	0.20	0.01	0.028	0.106	0.009	0.001	0.042	
17520	Nickel	0.25				0.20	0.20	98.4	0.10	0.10		0.50	0.10		0.10			
4	Nickel	0.037		0.0001		0.445	0.22	98.8	0.079	0.011		0.037	0.101		0.127	0.013		
1	Nickel	0.21		0.0001		0.049	0.12	98.3	0.104	0.15		0.99	0.03		0.03	0.002		
13593E	FeCr-binary	60.1							39.9									
50A	Nickel 200	0.04	0.023	0.002	0.002	0.11		99.8	0.01			0.01			0.02			
53A	Inconel <sup>®</sup> 600	7.62	0.063	0.009	0.001	0.32	0.15	76.1	15.1	0.02	0.05	0.11	0.25	0.02	0.12	0.002		
54A	Haynes 625	4.39	0.024	0.011	0.001	0.22	0.18	60.9	21.3	0.08	8.83	0.19	0.28	0.02	0.16	0.004	3.34	0.09
56A	Alloy 718	18.8	0.047	0.012	0.0012	0.11	0.14	52.2	18.5	0.04	3.08	0.25	1.01	0.03	0.56	0.005	5.10	0.04
57A	Alloy 750	7.06	0.05	0.005	0.0013	0.08	0.11	71.3	15.7	0.05	0.41	0.64	2.55	0.03	0.81	0.003	1.05	0.14
59A	INCO <sup>®</sup> 825	30.8	0.02	0.017	0.001	0.33	0.1	40.9	22.1	1.71	2.68	0.25	0.83	0.03	0.05	0.002	0.02	0.13
60A	RA 333	17.7	0.058	0.017	0.001	1.50	1.21	44.2	25.7	0.10	3.09	3.02	0.03	0.07	0.08	0.002	0.14	2.98
61A	Haynes 214	3.57	0.042	0.003	0.001	0.17	0.02	75.6	16.1	0.01	0.01	0.01	0.01	0.01	4.42	0.005	0.01	0.01
62A	Waspaloy	1.08	0.039	0.004	0.001	0.02	0.05	57.2	19.4	0.02	4.33	13.3	3.05	0.02	1.32	0.005	0.04	0.11
64A	Ultimet 1233	2.98	0.057	0.006	0.002	0.81	0.34	8.92	24.8	0.02	4.72	55.4	0.02		0.16			1.83
69A	Hast X	18.4	0.11	0.016	0.001	0.72	0.39	45.5	22.3	0.13	9.17	2.11	0.01	0.04	0.19	0.0005	0.12	0.82
BS925	Inconel <sup>®</sup> 925	26.9	0.011	0.016	0.002	0.50	0.11	43.5	20.8	1.74	3.00	0.34	2.20	0.03	0.17	0.002	0.23	0.47
BS187B	Carp. 20Cb3	39.1	0.018	0.021	0.015	0.78	0.63	33.8	19.8	3.12	2.05	0.19	0.002	0.077	0.035	0.0013	0.33	
BS600-4	Inconel <sup>®</sup> 600	8.40	0.034	0.007	0.004	0.20	0.22	75.9	14.7	0.08	0.002	0.09	0.20	0.023	0.06	0.006	0.015	
BS600-5	Inconel <sup>®</sup> 600	8.36	0.047	0.005		0.21	0.26	74.8	15.6	0.10	0.049	0.029	0.23	0.054	0.19	0.0018	0.03	
BS617	Inconel <sup>®</sup> 617	1.76	0.079	0.007		0.057	0.14	51.6	22.4	0.062	9.64	12.4	0.28	0.022	1.20	0.002	0.123	0.06
BS725	Inconel <sup>®</sup> 725	8.00	0.01	0.004	0.002	0.08	0.02	58.0	20.7	0.014	7.97	0.02	1.52	0.01	0.13	0.002	3.52	
BS825B	Incolloy <sup>®</sup> 825	35.1	0.024	0.013	0.0004	0.49	0.24	38.7	20.1	1.64	2.70	0.13	0.74	0.03	0.1	0.0004	0.04	
BS173	Alloy CCM	0.19	0.046	0.003	0.001	0.76	0.61	0.14	27.5	0.008	5.62	65.0	0.004	0.01	0.04	0.001	0.002	
BS161A	ASTM-A538C		0.01	0.0046	0.001	0.033	0.034	18.4	0.12	0.218	4.83	9.22	0.65	0.03	0.14	0.003		0.002
SS472	AISI 431	79.2	0.227	0.032	0.029	1.02	1.05	1.95	15.8		0.661							
SS350	Inconel <sup>®</sup> 713	1.50	0.138			0.019	0.11	70.8	13.4		4.29	0.338	0.87		5.97	0.013	2.17	0.094

together and the standard deviation of the five values of intensity was taken as  $\delta I_{EM}$ . Average of the five intensities was taken as  $I_{EM}$ . In this way, a prospective instrument drift during the experiment would deteriorate the random uncertainty of the intensities rather than the overall consistency of the calibration.

Sputter factors of the calibration samples were calculated as described under 2.1, using NIST 1761–1764 Low Alloy Steels and INCO 1, INCO 4, MBH 17520 and IARM 50A Nickel standards as the calibration base and assuming the sputter factor of nickel to be 1.59 relative to iron. This is the best estimate of the sputter factor of nickel relative to iron, as

resulting from earlier experiments. To avoid an excessive increase of uncertainty of the resulting sputter factors and, consequently, also of the calibration parameters, the step-wise calculations of the sputter factors with a changing calibration base, as described in ref. 5, were limited to three steps.

All calculations of the calibration parameters and the calculations in the consistency checks were performed according to the scheme in Fig. 1, together with the uncertainties associated with all parameters and variables. The results are presented below.

A summary of the calibration is given in Table 2. The A-type consistency table is given in Table 3. For the elements present at high concentrations, namely Fe, Ni, Cr and Co, relative errors of the predicted concentrations are plotted against concentrations in Fig. 3. Fig. 4 shows the random uncertainty of the predicted concentration divided by the error of the predicted concentration, plotted against concentration. Fig. 5 shows relative random uncertainty of the predicted concentration, plotted against concentration, for all analysed elements. All quantities shown in Figs. 3–5 were calculated in the A-mode.

#### 4. Discussion

Analytical performance of the calibration, measured using the A-mode  $(ERR)_E$  values (Table 2), gave values between 1 and 2 for most elements. This means that, at least for one half of the calibration samples, the deviations between the predicted and the certified concentrations range between a ‘typical uncertainty’ of the certified concentration and double that value. For the elements calibrated up to high concentrations, namely Fe, Ni, Cr and Co and, to some extent, also Mo, the  $(ERR)_E$  values are somewhat higher, due to the fact that the function  $\varepsilon(c)$  has very low values for high concentrations. This is because the certified concentrations of the matrix elements in most calibration samples are determined by the difference between 100% and the sum of concentrations of other elements, which leads to very low certified uncertainties, hardly achievable by actual measurements. For the somewhat worse

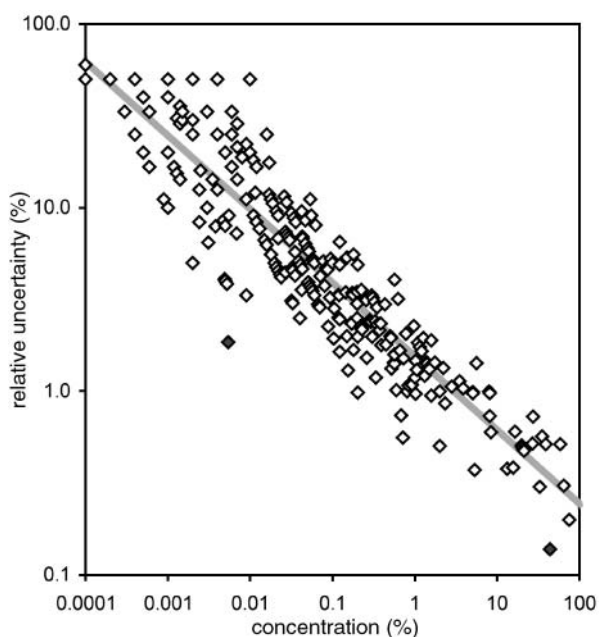


**Fig. 2** Relative uncertainty of the certified concentration as a function of concentration.

**Table 2** Overview of the calibration

Element	$\lambda/\text{nm}$	Calibration range		Number of calculated parameters	Degrees of freedom	BEC (ppm)	$(ERR)_E$ C-type	$(ERR)_E$ A-type
		Min (%)	Max (%)					
Fe	371.994	0.037	96	3	24	26	2.9	2.3
C	165.701	0.01	1.4	2	15	60	2.2	1.6
P	178.287	0.0001	0.04	5	20	874	1.5	1.5
S	180.731	0.0004	0.05	5	17	91	1.4	1.3
Mn	403.449	0.019	8.2	4	24	131	1.4	1.3
Si	288.158	0.02	4.0	5	18	151	5.4	4.4
Ni	349.296	0.14	99	3	26	412	3.3	3.0
Cr	267.716	0.01	40	5	24	336	2.7	3.1
Cr2	425.433	0.01	1.5	5	4	13.2		
Cu	327.396	0.008	3.1	4	18	63	1.2	1.1
Mo	386.411	0.002	10	4	20	105	3.6	3.6
Co	345.351	0.01	65	4	22	784	3.9	3.1
Ti	337.279	0.004	3.0	3	24	72	0.8	1.1
V	411.179	0.01	0.3	3	17	213	4.5	4.1
Al	396.152	0.009	6.0	3	21	11.4	2.2	1.8
B	208.959	0.0004	0.013	4	21	11.3	0.9	1.1
Nb	316.340	0.002	5.1	5	15	159	1.4	1.5
W	429.461	0.01	3.0	3	8	365	2.3	1.6

$(ERR)_E$  values in the case of Si and V, no credible explanation within the standard model has been found.

In the consistency tables such as Table 2, it is impossible to distinguish between deviations due to the inconsistency of the standard model and prospective deviations caused by wrongly certified concentrations. To suppress these, the median is used in the definition of  $(ERR)_E$  in eqn. (19), assuming that the vast majority of the certified concentrations are correct.

How well the calibration fits the standard model can be demonstrated, for example, by the fact that, for 16 out of 30 calibration samples, the difference between C-type and A-type sputter factors,  $q_M$ , is less than 1%; for 8 samples is less than 2%; and the remaining 6 calibration samples exhibit differences between 2 and 4%. Hence, it is realistic to say that a typical relative uncertainty of the sputter factors in this calibration is close to 1%. This result is much better than earlier results for

zinc alloys.<sup>11</sup> This is consistent with our experience from earlier studies that zinc-based materials are prone to bigger variations in the sputter factors than any other matrix.

The relative error of the predicted concentration in the A-mode as a function of concentration in the range of high concentrations is shown in Fig. 3. This plot shows how the error at high concentrations is affected by normalization [see eqn. (11) and point 2 relating to that equation].

In Fig. 4, the random uncertainty divided by the error of the predicted concentration is plotted against concentration for the same elements and in the same concentration range as in Fig. 3. Apparently, most measurements exhibit values less than 1, which means that the random uncertainty associated with the results is significantly smaller than the error of the predicted values. This indicates that the systematic errors for this calibration are more significant than the random errors.

**Table 3** A-type consistency table of the calibration with deviations expressed in the  $(ERR)_{EM}$  units defined by eqn. (18)

	Fe	C	P	S	Mn	Si	Ni	Cr	Cu	Mo	Co	Ti	V	Al	B	Nb	W
1761	-0.4	-1.6	-0.6	-0.4	0.7	0.8	1.1	-2.0	0.2	1.1	7.8	-2.6	-0.5	1.1	-1.1	-3.1	
1762	-0.5	-0.5	-0.5	-1.0	-1.3	4.2	2.3	-2.3	0.09	4.9	3.5	-0.5	1.0	0.2	0.8	0.03	
1763	-0.7	-0.6	-2.6	0.06	-0.2	2.9	3.2	-2.7	-0.7	5.0	1.6	0.2	-0.1	0.8	0.7	0.4	
1764	-0.1	-0.1	-1.4	-1.0	0.7	4.8	7.8	-3.3	-1.1	2.9	11	-2.6	-1.4	1.7	-1.2	-1.5	
17520	-2.0				-0.3	5.4	-0.8	0.6	-0.4		5.6	1.1		9.8			
4	-0.6		9.5		2.7	-5.6	-0.6	0.6	1.2		5.9	0.6		2.8	-1.2		
1	3.0		30		4.7	-12	-0.6	2.4	2.6		11	-1.1		2.3	-1.1		
13593E	2.8							-0.2									
50A	-1.2	4.9	7.5	2.4	-0.2		0.00	-2.6			3.4			-1.7			
53A	2.6	-1.0	4.0	-2.0	1.9	-4.1	-1.8	3.7	9.1	-4.7	-2.1	-0.6	-6.1	-8.1	-1.3	1.8	
54A	3.4	-2.8	-1.7	0.4	-2.3	-3.5	-3.4	3.9	-3.4	3.6	-3.6	-0.5	14	-2.9	0.5	-0.8	4.1
56A	-1.4	0.1	-3.6	1.4	-1.2	-7.4	3.8	-3.8	-14	-2.9	-1.7	-1.7	-0.6	0.1	-0.6	0.2	9.3
57A	2.1	6.1	-0.2	2.4	-2.7	3.1	-1.6	1.8	-2.0	-3.1	0.4	-0.03	-3.1	3.1	1.3	-0.8	0.8
59A	-7.0	-21	0.4	-1.2	0.4	-12	5.3	1.1	1.0	0.3	-0.4	0.3	16	-0.2	1.1	-6.3	-0.7
60A	-2.3	1.8	-0.8	-2.8	2.0	7.5	-6.7	9.9	-1.4	-1.1	-3.1	2.0	18	-2.3	6.4	4.2	-1.6
61A	3.2	-0.04	0.00	-1.6	-1.5	5.4	2.0	-3.6	7.8	-0.9	0.9	2.9	-4.5	-5.1	0.5	2.1	12
62A	2.7	-5.7	-0.4	0.00	1.2	-13	3.0	-2.0	-6.1	-9.5	0.5	0.2	-4.5	-1.5	1.4	-1.3	-1.5
64A	-2.3	0.5	1.8	1.3	-1.7	3.6	-5.1	12	1.0	-7.3	-2.4	-1.1		3.4			-8.9
69A	-3.2	0.6	1.2	-1.6	1.5	2.4	-4.4	5.4	-0.9	5.9	0.2	2.5	1.9	-2.4	-1.2	2.8	0.01
BS925	-7.2	-3.1	1.5	-1.3	-0.3	1.5	3.0	4.7	0.8	-1.4	-3.1	1.7	-0.3	1.4	2.9	0.1	-1.0
BS187B	-5.6	-17	1.4	9.9	1.6	-0.8	10	-5.0	1.5	-1.4	-1.5	-12	-0.5	0.6	-0.7	0.1	
BS600-4	0.03	-13	2.3	-0.9	0.05	-6.4	-2.4	6.7	0.8	-21	-3.7	2.6	-13	0.8	-0.1	1.8	
BS600-5	-0.7	-8.2	0.9		-0.6	-3.6	-1.3	4.7	0.3	-5.2	-7.6	1.0	-7.1	-0.1	-1.4	3.4	
BS617	0.6	0.8	0.4		-4.2	0.8	0.7	-0.7	-0.8	-3.8	1.4	-2.1	2.5	0.7	-0.3	-1.5	-4.0
BS725	9.8	-0.3	-3.9	-1.9	-4.6	-13	-1.1	-1.9	-15	0.1	-14	-1.0	7.0	-2.0	-3.7	-0.7	
BS825B	-9.0	-13	2.4	-0.7	-0.9	-4.5	12	-3.4	0.7	-2.4	-7.1	-1.1	6.1	-2.5	-0.7	7.7	
BS173	-3.5	2.6	-1.9	-2.0	-3.7	3.1	-4.8	4.8	2.8	-8.3	-0.9	-0.5	11	3.4	-0.4	-19	
BS161A		0.4	3.4	3.2	1.0	8.0	7.4	-2.9	0.4	6.7	8.0	3.0	-3.6	1.4	2.1		-101
SS472	1.5	-0.3	-0.3	-0.8	-0.2	7.4	3.0	-4.9		3.6							
SS350	5.4	-2.8			-5.1	2.0	-2.5	0.8		2.5	1.0	-0.1		1.9	0.3	-1.5	0.5

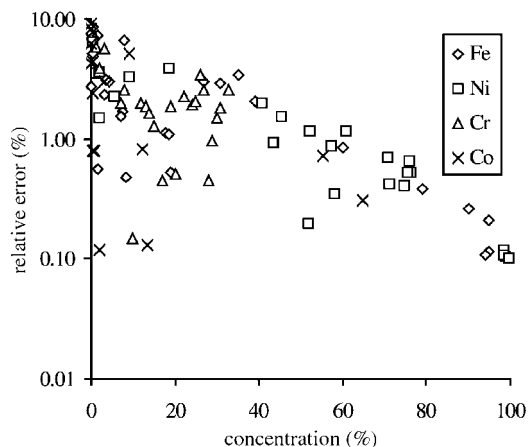


**Fig. 3** Relative deviation between the predicted (A-mode) and the certified concentrations (error) as a function of the certified concentration (matrix elements).

Because, supposedly, the calibration is correct within the standard model, this exposes limits of the standard model concerning its ability to describe the instrument response and predict the result. It is worth mentioning that the above statement depends on the quality of the instrumentation used; only with instruments providing data with a sufficiently low random uncertainty can systematic deviations from the calibration model be credibly revealed.

The plot in Fig. 5 shows how the random uncertainty of the predicted concentration depends on concentration. Although the spread in the random uncertainty spans over 1–2 orders of magnitude, the general trend towards increasing the relative random uncertainty with decreasing concentration is clearly apparent.

Finally, a remark about an important issue of statistical weighting: in the above described regression calculations, the following statistical weights were used:

$$w_{E,M} = 1 + k_E / (I_{E,M}^2 + 0.001) \quad (20)$$

where  $k_E$  is a constant specific for the element  $E$ . This weighting reflects the observed statistical distributions of the intensities in multiple analyses and assumes certain characteristics of the used instrument, e.g., settings of the gain (amplification of the signal) in different channels. Obviously, the determining factor for the statistical weighting is always the criterion of regression, i.e., the quantity that has to be minimized. As was mentioned above, the random uncertainty does not limit the analytical performance in this case: hence, it would be probably more

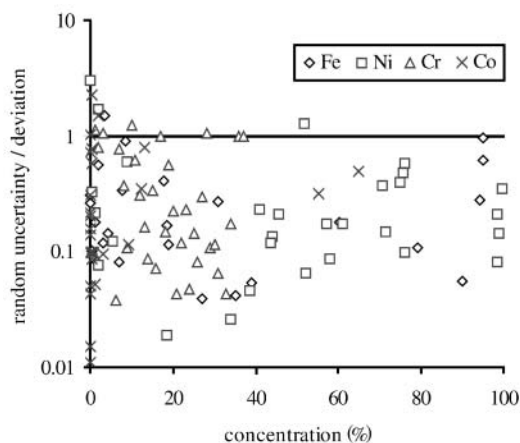


**Fig. 4** Random uncertainty of the predicted concentration (A-mode) divided by the deviation between the predicted and the certified concentration as a function of concentration.

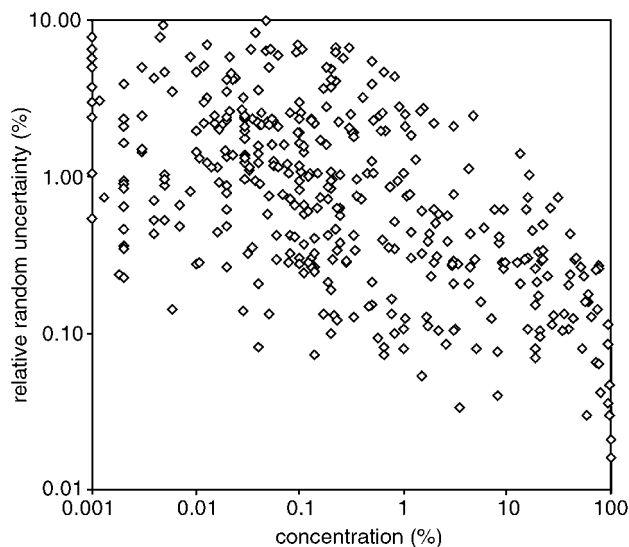


**Fig. 5** Relative random uncertainty of the predicted concentration (A-mode) as a function of the certified concentration.

appropriate to minimize, for example, the error expressed by the quantity,  $(ERR)_{EM}$ , and define the statistical weights using eqns. (17) and (18).

## 5. Conclusions

Propagation of uncertainty was analysed in multi-matrix calibrations by GD-OES. A formalism was developed to calculate uncertainties of the calibration parameters, sputter factors and predicted concentrations, and was applied to a calibration designed to analyse a wide range of materials, mostly nickel alloys.

In this calibration, statistically significant deviations from the standard model were found, although the achieved analytical performance was good according to the common criteria for multi-matrix methods.

Typical levels of uncertainty to be expected in the multi-matrix analysis by GD-OES were determined and may become a basis for further improvements of the calibration model, for a comparison between theoretical studies and the experiment, and to compare the analytical performance between GD-OES and other methods, between different experimental modifications of GD-OES and between different instruments.

Finally, the results presented here may be used as a basis for a proper choice of statistical weighting in regression calculations of the multi-matrix calibration.

## Acknowledgement

The author wishes to thank Mr. Horst Lehmkämer, LECO Instrumente GmbH., Germany, for the loan of some calibration samples used in this work.

## References

- 1 J. Takadoum, J. C. Pivin, J. Pons-Corbeau, R. Berneron and J. C. Charbonnier, *Surf. Interface Anal.*, 1984, **6**, 174.
- 2 A. Bengtson and M. Lundholm, *J. Anal. At. Spectrom.*, 1988, **3**, 879.
- 3 K. I. Suzuki, T. Ohtsubo and T. Watanabe, *Nippon Steel Technical Report*, 1987, p. 33.
- 4 Z. Weiss, *J. Anal. At. Spectrom.*, 1994, **9**, 351.
- 5 Z. Weiss, 'Multi-element Calibration', in *Glow Discharge Optical Emission Spectrometry*, ed. R. Payling, D. Jones and A. Bengtson, J. Wiley, New York, 1997, pp. 418–427.
- 6 Z. Weiss, *J. Anal. At. Spectrom.*, 1995, **10**, 891.
- 7 Z. Weiss, *J. Anal. At. Spectrom.*, 1997, **12**, 159.
- 8 A. Bengtson and S. Hånström, in *Proceedings of the ECICETAS*

- Conference on "Progress in Analytical Chemistry in the Steel and Metals Industries"*, Luxembourg, 1999, ISBN 92-828-6905-9, p. 47.
- 9 V. Hoffmann, lecture at the EC Thematic Network Analytical GDS Expert Meeting, BAM, Berlin, May 3–5, 2000.
  - 10 R. Payling and P. Chapon, lecture at the Midterm EC Thematic Network Analytical GDS Meeting, Kingston, July 20–22, 2000.
  - 11 Z. Weiss and P. Šmid, *J. Anal. At. Spectrom.*, 2000, **15**, 1485.
  - 12 J. R. Taylor, *An Introduction to Error Analysis*, University Science Books, Sausalito, California, 2nd edn., 1997, ISBN 0-935702-75-X.
  - 13 ASTM Standard E 1009-95: Standard Practice for Evaluating an Optical Emission Vacuum Spectrometer to Analyse Carbon and Low-Alloy Steel.